ACS EARTH AND SPACE CHEMISTRY

Article

Cite This: ACS Earth Space Chem. 2019, 3, 1966−1973

http://pubs.acs.org/journal/aesccq

Stable Carbon Isotopes of Fossil Plant Lipids Support Moderately High pCO_2 in the Early Paleogene

Taylor W. Chapman,[†] Ying Cui,*[,‡] and Brian A. Schubert[†]

[†]School of Geosciences, University of Louisiana at Lafayette, Lafayette, Louisiana 70504, United States

[‡]Department of Earth and Environmental Studies, Montclair State University, Montclair, New Jersey 07043, United States

Supporting Information

ABSTRACT: The atmospheric CO_2 concentration (pCO_2) affects the carbon isotope composition ($\delta^{13}C$) of plant tissue produced during photosynthesis. This observation has led to the suggestion that changes in the $\delta^{13}C$ value of bulk terrestrial organic matter (TOM) can be used to reconstruct pCO_2 on geologic time scales. It is possible, however, for bulk TOM to be affected by differential degradation that may affect the $\delta^{13}C$ value post-deposition and, therefore, bias estimates of pCO_2. Long-chain *n*-alkanes are commonly preserved in the fossil record and represent compound-specific biomarkers of higher order land plants, suggesting that their $\delta^{13}C$ values may provide a less biased estimate of pCO_2 than bulk TOM. Here, we report new pCO_2 estimates determined from published $\delta^{13}C$ data on long-chain, odd-numbered *n*-alkanes extracted from early Paleogene samples. During the early Paleogene, *n*-C_{27}, *n*-C_{29}, and *n*-C_{31} showed significantly higher net carbon isotope discrimination (Δ) compared to modern values ($p < 0.001$), consistent with moderately high CO_2 levels (average early Paleogene pCO_2 = 462 + 349/−162 ppm); *n*-C_{33} showed no significant change in discrimination compared to modern values ($p = 0.754$). Sensitivity analysis shows that independent knowledge on changes in plant taxa and mean annual precipitation can help improve the precision of our pCO_2 reconstruction. These results support background pCO_2 less than ∼3 times pre-industrial levels in the 10 million years leading up to the early Eocene climate optimum.

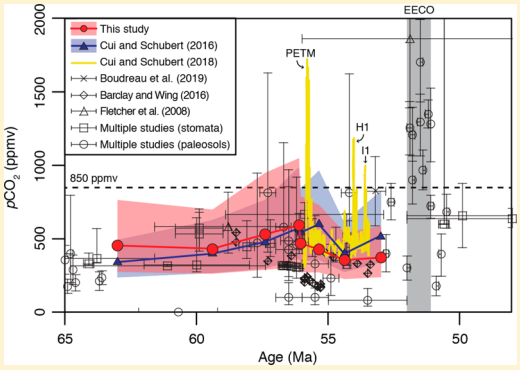

KEYWORDS: *carbon isotopes, early Eocene climate optimum, pCO_2, Paleogene, n-alkanes*

1. INTRODUCTION

It has long been known that both environmental conditions and plant taxon can affect the carbon isotope value ($\delta^{13}C$) of long-chain *n*-alkanes.[1−4] These observations have allowed workers to use the $\delta^{13}C$ value of *n*-alkanes to infer environmental and species change in both recent[5−7] and deep-time[8−11] studies. Researchers have also long suspected that the levels of atmospheric CO_2 (pCO_2) affect the $\delta^{13}C$ value of C_3 plant tissues.[12−14] The magnitude of this effect, however, has been poorly constrained and inconsistently applied,[15−20] and identification of this signal in the fossil record has proven difficult.[21,22] Laboratory experiments allowed for the effect of pCO_2 to be isolated from other environmental factors that are also known to affect the $\delta^{13}C$ value of plant tissues [e.g., water availability, temperature, light levels, and $\delta^{13}C$ value of atmospheric CO_2 ($\delta^{13}C_{atm}$)] and provided a unifying relationship for describing the response of carbon isotopes in C_3 plants at elevated pCO_2.[23] Subsequent work revealed that this response is consistent with the effects of photorespiration and mathematically independent of stomatal conductance and the photosynthetic rate.[24] Because photorespiration occurs downstream from stomatal diffusion, changes in net carbon isotope discrimination [$\Delta = (\delta^{13}C_{atm} - \delta^{13}C_{org})/(1 + \delta^{13}C_{org}/1000)$] under changing pCO_2 do not require any change in the ratio of intercellular CO_2 to atmospheric CO_2 (c_i/c_a).[24] As a result, c_i/c_a may be maintained across geologic time scales, despite changes in pCO_2 (for example, see section 3.2.2 within the study by Diefendorf and Freimuth[1]). There is now recognition for the need to account for changes in pCO_2 when interpreting bulk carbon isotope records within modern[25−30] and fossil[25,31−37] data sets and a clear expectation that the $\delta^{13}C$ value of individual plant biomarkers, such as leaf waxes (e.g., long-chain *n*-alkanes), should respond similarly to changing pCO_2.[23,38,39] To date, however, there has been no comparison of pCO_2 reconstructed using the $\delta^{13}C$ value of bulk terrestrial organic matter (TOM) versus long-chain *n*-alkanes in deep time, when diagenetic alteration may bias bulk $\delta^{13}C$ values.

Here, we focus on the early Paleogene (63−53 Ma), which contains an apparent disconnect between carbon cycle models that assume background pCO_2 of at least 750−1000 ppm,[40−42] and proxy data that indicate background pCO_2 = 356 + 145/−78 ppm ($n = 16$).[43] Because *n*-alkane $\delta^{13}C$ values are resistant to microbial degradation and diagenetic effects[44−48] and can be

Received: May 22, 2019
Revised: July 15, 2019
Accepted: July 19, 2019
Published: July 19, 2019

DOI: 10.1021/acsearthspacechem.9b00146
ACS Earth Space Chem. 2019, 3, 1966−1973

Table 1. Compiled Modern Angiosperm $\delta^{13}C_{n\text{-alkane}}$ Data (Mean ± 1σ), Adapted with Permission from Table E-1 of Ref 1[a]

reference	location	$\delta^{13}C_{n\text{-}C_{27}}$ (‰)	$\delta^{13}C_{n\text{-}C_{29}}$ (‰)	$\delta^{13}C_{n\text{-}C_{31}}$ (‰)	$\delta^{13}C_{n\text{-}C_{33}}$ (‰)
		Angiosperm			
Badewien et al.[94]	Angola	−34.0 ± 2.2	−34.7 ± 2.2	−35.8 ± 2.6	−36.8 ± 2.5
Bi et al.[95]	China	−35.5 ± 1.7	−35.2 ± 2.0	−35.9 ± 1.5	−36.5 ± 1.5
Chikaraishi and Naraoka[82]	Gunma, Japan	−34.3 ± 0.9	−33.7 ± 0.6	−33.5 ± 0.1	−33.3 ± 1.6
Collister et al.[96]	England	−32.4 ± 0.6	−33.3 ± 1.4	−35.4 ± 2.2	−36.1 ± 1.8
Conte et al.[97]	Canada	−33.9 ± 2.4	−33.6 ± 1.6	−32.8 ± 1.1	−33.1 ± 1.7
Diefendorf et al.[50]	Wyoming, U.S.A.	−32.0 ± 2.5	−29.3 ± 0.0	−31.4 ± 2.6	−32.5 ± 0.0
Diefendorf et al.[50]	Pennsylvania, U.S.A.	−33.4 ± 1.5	−33.4 ± 2.1	−33.7 ± 2.0	−33.8 ± 1.6
Duan and He[98]	China	−30.6 ± 2.9	−32.1 ± 1.5	−35.8 ± 1.6	
Garcin et al.[99]	Cameroon	−33.3 ± 2.5	−33.9 ± 2.5	−34.1 ± 2.5	−34.6 ± 3.0
Krull et al.[100]	Australia	−34.3 ± 0.9	−35.7 ± 0.1	−34.0 ± 2.9	
Lockheart et al.[3]	England	−30.9 ± 1.9			
Vogts et al.[68]	Africa	−32.9 ± 2.1	−34.4 ± 2.7	−34.7 ± 2.6	−34.7 ± 2.4
average $\delta^{13}C_{t=0}$		−33.1 ± 2.0	−33.6 ± 1.7	−34.3 ± 2.1	−34.6 ± 2.0
		Gymnosperm			
Bi et al.[95]	China		−30.1 ± 0.0	−30.5 ± 0.0	−29.1 ± 0.0
Chikaraish and Naraokai[82]	Japan	−33.0 ± 1.2	−32.3 ± 0.7	−32.2 ± 1.2	−31.5 ± 1.7
Diefendorf et al.[50]	Wyoming, U.S.A.		−32.2 ± 0.0	−31.5 ± 0.0	−30.5 ± 0.0
Diefendorf et al.[50]	Pennsylvania, U.S.A.	−30.1 ± 0.9	−29.9 ± 1.3	−30.5 ± 1.4	−29.5 ± 2.7
Diefendorf et al.[50]	California, U.S.A.	−33.3 ± 2.8	−33.0 ± 2.6	−33.4 ± 2.6	−32.4 ± 2.5
average $\delta^{13}C_{t=0}$		−32.1 ± 1.8	−31.5 ± 1.3	−31.6 ± 1.4	−30.6 ± 1.8

[a]Excludes lianas (vines), understory plants with $\delta^{13}C_{bulk} < -31.5$‰ (after Kohn[81]), sites with $n < 2$ plants, and one *Ficus ottoniifolia* and one *Englerina gabonensis*, which had exceptionally low $\delta^{13}C$ values likely caused by local source CO_2 effects.[68]

Table 2. Values Used To Calculate $pCO_{2(t)}$ and Associated Uncertainty

input variable (eq 1)	input value	uncertainty (±1σ)	source
$pCO_{2(t=0)}$ (ppm)	377	10	Keeling et al.[28]
$\delta^{13}C_{CO_2(t=0)}$ (‰)	−8.1	0.1	Keeling et al.[28]
$\delta^{13}C_{CO_2(t)}$ (‰)	variable	0.5	Tipple et al.[63]
$\delta^{13}C_{n\text{-}C_{27}(t=0)}$ (‰)	−33.0	2.0	Table 1[a]
$\delta^{13}C_{n\text{-}C_{29}(t=0)}$ (‰)	−33.4	1.7	Table 1[a]
$\delta^{13}C_{n\text{-}C_{31}(t=0)}$ (‰)	−34.0	2.1	Table 1[a]
$\delta^{13}C_{n\text{-}C_{33}(t=0)}$ (‰)	−34.2	1.9	Table 1[a]
$\delta^{13}C_{org(t)}$ (‰)	variable	∼0.1	Diefendorf et al.[56]
A	28.26	0	Schubert and Jahren[23,25,101]
B	0.22	0.028	Cui and Schubert[36]
C	median value determined in Monte Carlo analysis	determined in Monte Carlo analysis	Cui and Schubert[36]

[a]Calculated assuming a 90:10 ratio of angiosperms/gymnosperms.

traced to a particular class of plants (i.e., vascular land plants[1,49,50]), we sought to apply changes in the $\delta^{13}C$ values of long-chain *n*-alkanes (*n*-C_{27}, *n*-C_{29}, *n*-C_{31}, and *n*-C_{33}) toward providing improved estimates of pCO_2 across this time interval. We compare these estimates to those determined using bulk TOM from the same sediments[36] and other independent pCO_2 proxies, including stomata, boron isotopes, liverworts, and paleosols.[43,51] These data highlight a clear model−proxy divide over background pCO_2 during the early Paleogene.

2. METHODS

Experiments growing plants under controlled environmental conditions and a wide range of pCO_2 revealed the following general hyperbolic relationship between the Δ value and pCO_2:[23]

$$\Delta = [(A)(B)(pCO_2 + C)]/[(A) + (B)(pCO_2 + C)] \quad (1)$$

Water availability also affects Δ values but does not affect the slope of this relationship (change in Δ per parts per million of pCO_2);[23,24,36] therefore, pCO_2 at any time t ($pCO_{2(t)}$) can be quantified on the basis of changes in the Δ value [i.e., Δ(Δ)] between the time period of interest (Δ_t) and a reference period with known pCO_2 ($\Delta_{t=0}$) by solving the following equation (after Schubert and Jahren[25]):

$$\Delta(\Delta) = \Delta_t - \Delta_{t=0} = [(A)(B)(pCO_{2(t)} + C)] /[(A) + (B)(pCO_{2(t)} + C)] - [(A)(B)(pCO_{2(t=0)} + C)] /[(A) + (B)(pCO_{2(t=0)} + C)] \quad (2)$$

where $A = 28.26$, $B = 0.22$, and C is determined via Monte Carlo analysis following Cui and Schubert.[36] Because plant carbon isotope values vary on the basis of species and growing conditions,[52−54] eq 2 instead of eq 1 (cf. eq 1[55,56]) should be used to calculate pCO_2. The applicability of eq 2 as a proxy for pCO_2 was validated through a comparison to ice core data[25] and

DOI: 10.1021/acsearthspacechem.9b00146
ACS Earth Space Chem. 2019, 3, 1966−1973

has been applied to deep-time settings.[32,34,36] Uncertainty in determination of $pCO_{2(t)}$ (eq 2) is a function of uncertainty in the curve fitting parameters (A, B, and C) and estimation of Δ_t, $\Delta_{t=0}$, and $pCO_{2(t=0)}$.[36]

Because eq 2 uses relative changes in the Δ value [i.e., Δ(Δ)] to calculate $pCO_{2(t)}$, a robust estimate of $\Delta_{t=0}$ at known pCO_2 (i.e., $pCO_{2(t=0)}$) is critical to the accuracy of the proxy. Here, we use modern data for $\Delta_{t=0}$ within eq 2 (Table 1 and references therein), because both pCO_2 and $\delta^{13}C_{atm}$ are particularly well-constrained (Table 2[28]). Because gymnosperms show significantly lower Δ values than angiosperms, even when growing under the same conditions,[53,57] we compiled angiosperm and gymnosperm $\Delta_{t=0}$ data separately (Table 1). Laboratory experiments showed that the use of a multispecies assemblage improves the accuracy of the proxy over calculations that use only a single species.[58] The $\Delta_{t=0}$ data were calculated from the $\delta^{13}C$ value of long-chain n-alkanes from modern plants (n-C_{27}, n-C_{29}, n-C_{31}, and n-C_{33}) and the modern $\delta^{13}C_{atm}$.[28]

Eight early Paleogene (63−53 Ma) fluvial sites have been studied for long-chain n-alkane carbon isotopes from the carbonaceous rocks that are dated at 52.98, 54.37, 55.34, 56.04, 56.1, 57.39, 59.39, and 63 Ma.[56] The paleotemperature at the eight sites was estimated to be 11−22 °C, while the reconstructed mean annual precipitation did not vary substantially across the 10 million year time interval [from 1090 + 470/−330 to 1730 + 750/−520 mm year^{-1} ± 1 standard error (SE)].[56] The temperature change does not exert a strong control on Δ_t according to studies on modern soil organic matter[59−61] but may play a role in plants growing under high temperature and water stress.[62] The Bighorn Basin sites are associated with moderate temperature and semi-humid to humid climate in the early Paleogene, making them ideal to study the pCO_2 effect on carbon isotope fractionation.

Carbon isotope discrimination data for the early Paleogene (Δ_t) were calculated from long-chain n-alkane $\delta^{13}C$ values reported within Table A-1 from Diefendorf et al.[56] for the Bighorn Basin (Wyoming, U.S.A.) and the $\delta^{13}C_{atm}$ data from Tipple et al.[63] Following Diefendorf et al.,[64] we assumed a 90:10 ratio of angiosperms/gymnosperms at the fossil sites[65,66] and recognize that, because angiosperms produce up to 200 times more n-alkanes than gymnosperms, they will likely dominate the paleorecords of n-alkanes in many environments.[50] Angiosperm contributions are likely limited, however, when studying older (i.e., pre-Cenozoic) sites[67] or sites that are dominated by evergreen and deciduous conifers (e.g., boreal forests). Because the relative abundance of angiosperms to gymnosperms can vary through time and across diverse locations, we present a sensitivity analysis at 10% intervals across the entire range of possible angiosperm abundances (0−100%) to illustrate the effect that the plant community change can have on the calculation of $pCO_{2(t)}$.

All other input values and their associated uncertainties for pCO_2 calculations are listed in Table 2. All results are reported as the median of 10 000 randomly generated pCO_2 estimates using the R code provided in the Supporting Information; uncertainty is reported as 1 standard deviation (or 68% confidence interval), unless noted.

3. RESULTS

On average, carbon isotope discrimination values were significantly greater for the Paleogene data compared to modern data for the three most dominant chain lengths, n-C_{27}, n-C_{29}, and n-C_{31} [$\Delta(\Delta)_{n\text{-}C_{27}}$ = 0.72 ± 0.93‰, n = 43, and Welch two-sample t test, $p < 0.001$; $\Delta(\Delta)_{n\text{-}C_{29}}$ = 0.94 ± 1.00‰, n = 42, and $p < 0.001$; and $\Delta(\Delta)_{n\text{-}C_{31}}$ = 0.71 ± 1.05‰, n = 41, and $p < 0.001$], but no significant difference was observed for n-C_{33} [$\Delta(\Delta)_{nC_{33}}$ = −0.18 ± 1.21‰, n = 21, and p = 0.754] (Figure 1). Using eq 2, we calculated average pCO_2 during the early Paleogene (i.e., $pCO_{2(t)}$ = 449 + 334/−157 ppm; n = 147), with the highest estimates for the dominant n-alkanes (n-C_{27}, n-C_{29}, and n-C_{31}) and lower estimates when using n-C_{33} (Figure 2). Estimates of pCO_2 based on n-C_{27}, n-C_{29}, and n-C_{31} are not statistically different (Wilcoxon rank sum test, $p > 0.6$) but do differ significantly from results based on n-C_{33} (Welch two-sample t test, $p < 0.001$). Excluding the results of n-C_{33}, the average pCO_2 during the early Paleogene is calculated as 462 + 349/−162 ppm (n = 126).

4. DISCUSSION

The positive Δ(Δ) values determined for n-C_{27}, n-C_{29}, and n-C_{31} (Figure 1) are consistent with laboratory experiments[23] and field observations,[38] showing an increase in $\Delta_{n\text{-alkanes}}$ with increasing pCO_2. We note that n-C_{27}, n-C_{29}, and n-C_{31} are also the dominant chain lengths produced by C_3 vascular plants[68] and are best represented in the fossil data set; the least abundant chain length studied here (n-C_{33}) showed no significant change in discrimination overall (Figure 1). In modern plants, significant abundances of n-C_{33} are generally limited to Cupressaceae (i.e., cypress) and C_4 plants[1] but have also been found in higher concentrations within members of the Ericaceae family, including *Calluna vulgaris*[69] and a limited number of *Rhododendron* spp.[70] Given the early Paleogene age for the sites, C_4 plant contributions are unlikely. Ericaceae fossils of similar age have been reported in the literature[71] but none from the sites examined here. Additional experiments to test the effect of pCO_2 across the entire suite of long-chain n-alkanes (i.e., n-C_{25} and above) would help elucidate if the response observed for n-C_{27}, n-C_{29}, and n-C_{31} should be expected consistently across other chain lengths.

In addition to pCO_2, the Δ value of both n-alkanes and bulk TOM can also be affected by changes in the temperature[72] and mean annual precipitation (MAP)[56,65,66] across the 10 million year period of study. These changes in climate affect the

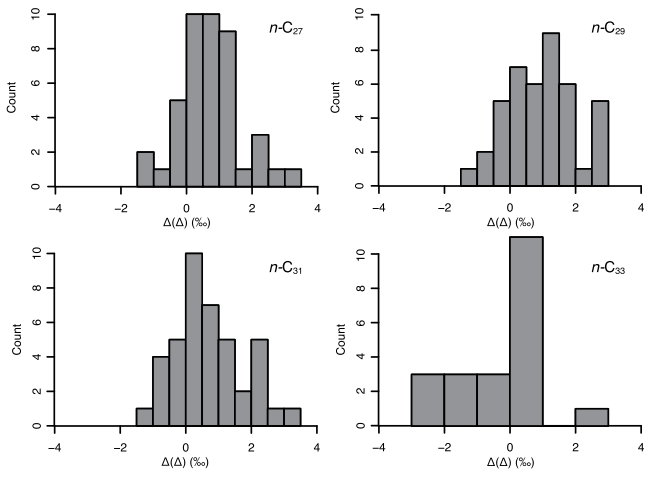

Figure 1. Changes in discrimination between the Paleogene (Δ_t) and modern ($\Delta_{t=0}$) [$\Delta(\Delta) = \Delta_t - \Delta_{t=0}$] for n-C_{27}, n-C_{29}, n-C_{31}, and n-C_{33}. The average Δ(Δ) value is significantly >0‰ for n-C_{27}, n-C_{29}, and n-C_{31} ($p < 0.001$) but not for n-C_{33} (p = 0.78).

DOI: 10.1021/acsearthspacechem.9b00146
ACS Earth Space Chem. 2019, 3, 1966−1973

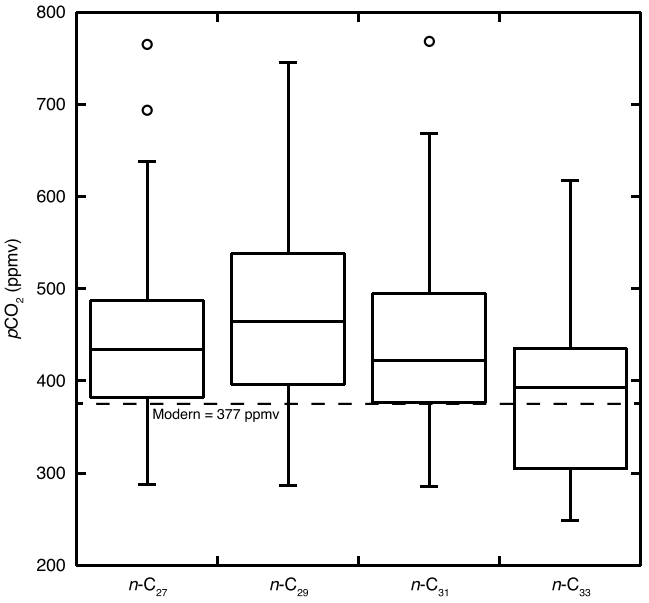

Figure 2. Early Paleogene $pCO_{2(t)}$ determined from the Δ value of *n*-alkanes (eq 2): $pCO_{2(n\text{-}C_{27})}$ = 451 + 350/−161 (*n* = 43), $pCO_{2(n\text{-}C_{29})}$ = 479 + 315/−156 (*n* = 42), $pCO_{2(n\text{-}C_{31})}$ = 454 + 383/−169 (*n* = 41), and $pCO_{2(n\text{-}C_{33})}$ = 377 + 251/−127 (*n* = 21). Individual pCO_2 estimates are presented in Table S1 of the Supporting Information.

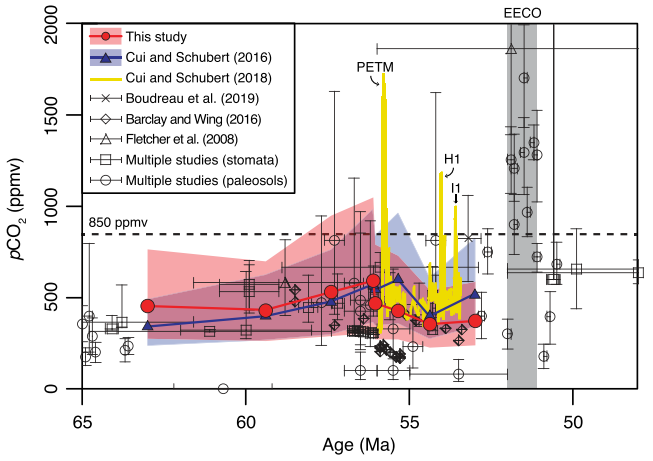

Figure 3. Evolution of pCO_2 across the early Paleogene. Note similar pCO_2 estimates obtained using $\Delta_{n\text{-alkane}}$ (red; this study) and Δ_{TOM} (blue; Cui and Schubert[36]). A comparison to other published studies (refs 43, 51, 83, and 102 and references therein) reveals that pCO_2 likely did not exceed ∼850 ppm (dashed line), with the exception of geologically brief hyperthermals (e.g., PETM, H1, and I1[34]) and a 1 Myr interval spanning the early Eocene climate optimum (52−51 Ma, gray shaded region). For clarity, median values without uncertainty are shown from Cui and Schubert.[34] Stomata and paleosol studies were compiled by Foster et al.[43]

photosynthetic rate and stomatal conductance[73−76] and, therefore, affect the $\delta^{13}C$ values of plant tissue[77] and estimates of pCO_2. Changes in the paleotemperature in the Paleogene,[78,79] however, are unlikely to affect the $\delta^{13}C$ records of the terrestrial sedimentary organic matter because $\delta^{13}C$ values of soil organic matter are not strongly affected by the temperature in modern environments.[59,60] MAP, on the other hand, has been considered to be an important factor that affects $\delta^{13}C$ values of soil organic matter in both modern and paleosettings.[22,59,80] Variability in the $\delta^{13}C$ value of modern *n*-alkanes reported here (1σ = 1.7−2.1‰; Table 2) is similar to but larger than that reported previously for bulk leaf tissue (1.6‰[81]) and is consistent with the substantial effect that climate and plant type has on the $\delta^{13}C$ value.[54,82] MAP influences the precision of our pCO_2 reconstruction and represents the largest source of uncertainty in our calculation of $pCO_{2(t)}$.[36] The error window presented in Figure 3 therefore represents the likely range of pCO_2 conditions across 63−53 Ma. We note, however, that confidence in the median values can be improved, provided independent knowledge of climate or plant taxa change.

Leaf margin analysis indicates MAP using at the Bighorn Basin ranges from 1090 to 1730 mm year^{-1} between 52.98 and 63 Ma.[65,66] To account for the carbon isotope discrimination incurred as a result of changes in MAP from 52.98 to 63 Ma, we adopted the logarithmic relationship between $\delta^{13}C$ and MAP reported by Kohn[81] for a global data compilation of modern leaves (for MAP < 1000 mm year^{-1}, the MAP effect on $\delta^{13}C$ is from −0.2 to −0.5‰ per 100 mm; for 1000 < MAP < 2000 mm year^{-1}, the MAP effect on $\delta^{13}C$ is from −0.1 to −0.2‰ per 100 mm) while holding altitude and latitude constant. The equation used to perform the MAP correction is as follows:

$$\delta^{13}C_{corrected} = \delta^{13}C_{raw} + (-5.61)\log_{10}(MAP_0 + 300) - (-5.61)\log_{10}(MAP_t + 300) \quad (3)$$

where $\delta^{13}C_{corrected}$ is the $\delta^{13}C$ value after accounting for MAP changes, $\delta^{13}C_{raw}$ is the original $\delta^{13}C$ values reported by Diefendorf et al.,[56] MAP_0 is the MAP at 63 Ma (i.e., 1200 mm year^{-1}), and MAP_t is the MAP at the remaining time slices. We observe no more than 95 ppm (∼16%) difference in pCO_2 at any time point when accounting for changes in MAP (Figure 4), and all MAP-corrected estimates fall within our original uncertainty window. This correction serves to reduce uncertainty in reconstructed pCO_2 by reducing uncertainty in $\Delta_{t=0}$ within eq 2 (average biome level uncertainty = 1.2‰ for angiosperms[54]) and reinforces our conclusion for pCO_2 of less than ∼3 times pre-industrial levels for the 10 million years prior to the early Eocene climate optimum.

The levels of CO_2 determined here assume that angiosperms dominate the $\delta^{13}C$ signal of *n*-alkanes preserved here (i.e., 90%

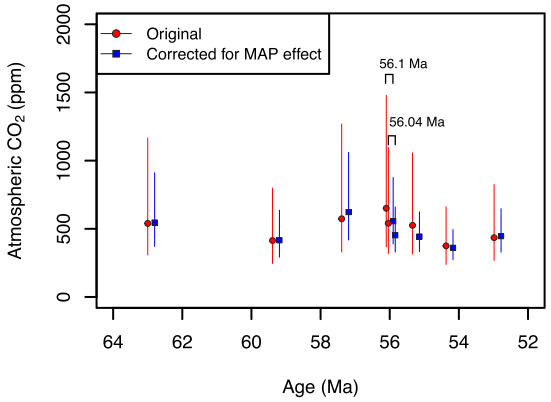

Figure 4. Effect of the MAP on the calculation of pCO_2 using $n\text{-}C_{31}$. Correcting $\delta^{13}C_t$ values for changes in MAP (eq 3) results in pCO_2 within 16% of uncorrected values for all time slices, but the effects are not significant. Note that constraint on MAP reduces uncertainty in reconstructed pCO_2. Blue (MAP-corrected) and red (no correction) data points are offset to avoid overlap.

DOI: 10.1021/acsearthspacechem.9b00146
ACS Earth Space Chem. 2019, 3, 1966−1973

angiosperm/10% gymnosperm). To assess the effect of the angiosperm/gymnosperm ratio on our calculated pCO_2, we calculated $pCO_{2(t)}$ across the entire range of potential scenarios, ranging from 100% angiosperm to 100% gymnosperm (Figure 5). While recognizing that a gymnosperm-dominated signal is unlikely,[50,64] we find that, for the dominant chain lengths, our estimate of $pCO_{2(t)}$ increases by no more than ~85 ppm, even if one assumes as much as a 50% contribution by gymnosperms to the $\delta^{13}C$ signal (in comparison to our preferred value of 10% gymnosperm). This analysis shows that, if the angiosperm contribution was lower than assumed (i.e., <90%), then our pCO_2 estimates reported here might be biased low and, therefore, represent minimum levels; however, the effect of this value on our pCO_2 result is relatively small (~20 ppm) across the likely range of angiosperm contributions (85–100%[56]). Thus, plant taxa and climate have similarly small effects on the pCO_2 reconstruction reported here.

The new early Paleogene pCO_2 estimates determined here using n-C_{27}, n-C_{29}, and n-C_{31} (462 + 349/−162 ppm; n = 126) are similar to previous estimates based on Δ_{TOM} (482 + 280/−170 ppm; n = 75[36]), paleosol carbonate (577 + 227/−152 ppm; n = 35), plant stomata (430 + 79/−52 ppm; n = 30), and recently revised ginkgo-based plant stomata[51] (297 ppm; n = 20; no uncertainty estimates are available) but notably lower than a single estimate based on the boron isotope composition of well-preserved planktonic Foraminifera (1400 ± 235 ppm; n = 1; Figure 3 and references therein). Recent work suggests that this latter value, which appears to be an outlier among the other proxy estimates, is likely biased high by more than 500 ppm,[83] bringing this value more in line with other proxy values. A total of 7 of the 10 highest pCO_2 estimates reported for the entire Cenozoic occur later within the Eocene, all within a relatively short interval from 52 to 51 Ma[43] (Figure 3). These very high levels of pCO_2 coincide with the peak of the early Eocene climate optimum, as indicated by oxygen isotope measurements of foraminifera;[84,85] however, there remains no proxy evidence for early Paleogene pCO_2 > 850 ppm prior to the early Eocene climate optimum, with the exception of the relatively brief Paleocene–Eocene thermal maximum (PETM).[32,34,86]

Unlike $\Delta_{n\text{-alkanes}}$, Δ_{TOM} can be further affected by diagenesis and mixing of inputs from algae and vascular land plants, leading to the distortion of the preserved Δ_{TOM} signal.[49,87] However, the excellent agreement between the levels of pCO_2 determined here using $\Delta_{n\text{-alkane}}$ compared to levels calculated previously using Δ_{TOM}[36] (Figure 3) suggests that the bulk TOM at these sites was likely not meaningfully affected by post-depositional or preservation factors.

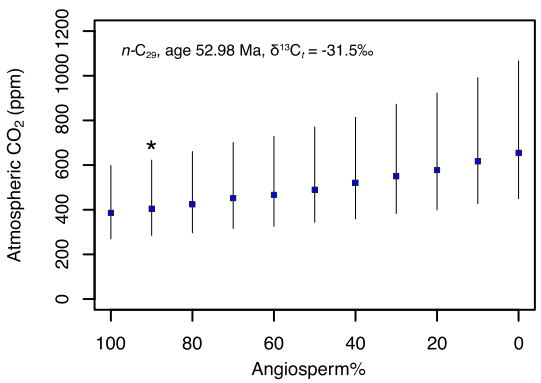

Figure 5. Effect of the angiosperm/gymnosperm ratio on calculation of pCO_2. The preferred result (90% angiosperm, after Diefendorf et al.[56]) is marked with an asterisk.

The similarities in pCO_2 reconstructed using $\Delta_{n\text{-alkane}}$ compared to Δ_{TOM} suggest that both substrates are providing similar paleoenvironmental information and chemical extractions of n-alkanes from bulk TOM might not be necessary for all settings. Furthermore, we see no reduction in the range of pCO_2 estimates calculated using $\Delta_{n\text{-alkane}}$ versus Δ_{TOM}, consistent with the similar $\delta^{13}C$ variability seen across these two substrates. The lack of any significant difference in pCO_2 calculated using $\Delta_{n\text{-alkane}}$ versus Δ_{TOM} (Figure 3) is consistent with strong correspondence between the two substrates; biosynthetic fractionation (ε) between $\Delta_{n\text{-alkane}}$ and Δ_{TOM} remained consistent across all samples analyzed.[56] Measurement of ε values ($\Delta_{n\text{-alkane}} - \Delta_{TOM}$) in a subset of fossil samples could therefore be used to assess diagenetic effects through comparison to ε values from modern, unaltered samples. Deviations in fossil ε values compared to modern values might indicate bias in Δ_{TOM} as a result of diagenesis or source mixing: for such sites, we recommend measurement of $\Delta_{n\text{-alkane}}$ or correction of Δ_{TOM} values for the effects of degradation and/or source mixing.[49]

5. CONCLUSION

These new pCO_2 estimates based on changes in carbon isotope discrimination of long-chain n-alkanes are consistent with available proxy data, including independent pCO_2 proxies (e.g., paleosol carbonate, plant stomata, and fossil liverworts) and previous estimates based on bulk TOM.[32,36] In contrast to expectations, we saw no obvious improvement in our pCO_2 data determined using n-alkanes versus TOM, suggesting good preservation of the original $\delta^{13}C$ signal within the fossil TOM. Measurement of ε ($\Delta_{n\text{-alkane}} - \Delta_{TOM}$) for a subset of samples could be used to assess potential diagenetic effects that might bias pCO_2 determined from Δ_{TOM}; here, fossil ε values were previously determined to be similar to modern values,[56] consistent with the similar pCO_2 estimates determined for $\Delta_{n\text{-alkane}}$ and Δ_{TOM}.

Changes in discrimination calculated here were relatively small and consistent with the stable, slightly elevated pCO_2 indicated by other proxies; however, significantly greater changes in discrimination have been recorded at geologically brief hyperthermal events, consistent with larger increases in pCO_2.[32,34,101] There is potential for the pCO_2 results reported here to be biased low by up to ~85 ppm if one assumes that gymnosperms accounted for as much as 50% of the n-alkane inputs; however, this bias is small compared to the large sample variability in the modern and fossil data sets and is insufficient to resolve the proxy–model divide surrounding early Paleogene pCO_2.[88,89] Likewise, changes in MAP had only a small effect on the pCO_2 calculated here; however, pCO_2 estimates at drier sites are expected to be more sensitive to changing MAP. Finally, we note that this proxy is relevant to all evolutionary time scales that include C_3 land plants;[24] the period studied here is well before the period of global C_4 grassland expansion of ~7–8 Ma.[81] The wide applicability of this proxy and the prevalence of long-chain n-alkanes within sedimentary organic matter of Cenozoic,[10,90,91] Mesozoic,[11,92] and Paleozoic[93] age suggest great potential for using $\Delta_{n\text{-alkanes}}$ values to reconstruct pCO_2 in the fossil record. Despite the influences of the changes in plant taxa and MAP on carbon isotope fractionation of C_3 land plants, we suggest that the precision of pCO_2 reconstruction in the past can be improved by independent knowledge of plant taxa and MAP.

DOI: 10.1021/acsearthspacechem.9b00146
ACS Earth Space Chem. 2019, 3, 1966–1973

■ ASSOCIATED CONTENT

Supporting Information

The Supporting Information is available free of charge on the ACS Publications website at DOI: 10.1021/acsearthspacechem.9b00146.

R code and input files to calculate pCO_2 and its uncertainty for n-C_{27}, n-C_{29}, n-C_{31}, and n-C_{33} and pCO_2 and its uncertainty calculated from long-chain n-alkanes in this study (Table S1) (ZIP)

■ AUTHOR INFORMATION

Corresponding Author

*E-mail: cuiy@montclair.edu and/or cuiying00@gmail.com.

ORCID

Ying Cui: 0000-0003-1057-4369

Notes

The authors declare no competing financial interest.

■ ACKNOWLEDGMENTS

This research was supported by the United States National Science Foundation (Award EAR-1603051) and the National Science Foundation of China (Grant 41888101).

■ REFERENCES

(1) Diefendorf, A. F.; Freimuth, E. J. Extracting the most from terrestrial plant-derived n-alkyl lipids and their carbon isotopes from the sedimentary record: A review. *Org. Geochem.* **2017**, *103*, 1−21.

(2) Ladd, S. N.; Sachs, J. P. Positive correlation between salinity and n-alkane $\delta^{13}C$ values in the mangrove Avicennia marina. *Org. Geochem.* **2013**, *64*, 1−8.

(3) Lockheart, M. J.; Van Bergen, P. F.; Evershed, R. P. Variations in the stable carbon isotope compositions of individual lipids from the leaves of modern angiosperms: Implications for the study of higher land plant-derived sedimentary organic matter. *Org. Geochem.* **1997**, *26* (1), 137−153.

(4) Rieley, G.; Collier, R. J.; Jones, D. M.; Eglinton, G.; Eakin, P. A.; Fallick, A. E. Sources of sedimentary lipids deduced from stable carbon-isotope analyses of individual compounds. *Nature* **1991**, *352*, 425−427.

(5) Aichner, B.; Wilkes, H.; Herzschuh, U.; Mischke, S.; Zhang, C. Biomarker and compound-specific $\delta^{13}C$ evidence for changing environmental conditions and carbon limitation at Lake Koucha, eastern Tibetan Plateau. *Journal of Paleolimnology* **2010**, *43* (4), 873−899.

(6) Huang, Y.; Street-Perrott, F.; Perrott, R.; Metzger, P.; Eglinton, G. Glacial-interglacial environmental changes inferred from molecular and compound-specific $\delta^{13}C$ analyses of sediments from Sacred Lake, Mt. Kenya. *Geochim. Cosmochim. Acta* **1999**, *63* (9), 1383−1404.

(7) Sinninghe Damsté, J. S.; Verschuren, D.; Ossebaar, J.; Blokker, J.; van Houten, R.; van der Meer, M. T.; Plessen, B.; Schouten, S. A 25,000-year record of climate-induced changes in lowland vegetation of eastern equatorial Africa revealed by the stable carbon-isotopic composition of fossil plant leaf waxes. *Earth Planet. Sci. Lett.* **2011**, *302* (1−2), 236−246.

(8) Handley, L.; Pearson, P.; McMillan, I.; Pancost, R. Large terrestrial and marine carbon and hydrogen isotope excursions in a new Paleocene/Eocene boundary section from Tanzania. *Earth Planet. Sci. Lett.* **2008**, *275* (1−2), 17−25.

(9) Ruhl, M.; Bonis, N. R.; Reichart, G. J.; Damsté, J. S. S.; Kürschner, W. M. Atmospheric carbon injection linked to end-Triassic mass extinction. *Science* **2011**, *333* (6041), 430.

(10) Tipple, B. J.; Pagani, M. A 35Myr North American leaf-wax compound-specific carbon and hydrogen isotope record: Implications for C_4 grasslands and hydrologic cycle dynamics. *Earth Planet. Sci. Lett.* **2010**, *299* (1), 250−262.

(11) Whiteside, J. H.; Olsen, P. E.; Eglinton, T.; Brookfield, M. E.; Sambrotto, R. N. Compound-specific carbon isotopes from Earth's largest flood basalt eruptions directly linked to the end-Triassic mass extinction. *Proc. Natl. Acad. Sci. U. S. A.* **2010**, *107* (15), 6721−6725.

(12) Feng, X.; Epstein, S. Carbon isotopes of trees from arid environments and implications for reconstructing atmospheric CO_2 concentration. *Geochim. Cosmochim. Acta* **1995**, *59* (12), 2599−2608.

(13) Körner, C.; Farquhar, G.; Wong, S. Carbon isotope discrimination by plants follows latitudinal and altitudinal trends. *Oecologia* **1991**, *88* (1), 30−40.

(14) Krishnamurthy, R.; Epstein, S. Glacial-interglacial excursion in the concentration of atmospheric CO_2: Effect in the $^{13}C/^{12}C$ ratio in wood cellulose. *Tellus, Ser. B* **1990**, *42* (5), 423−434.

(15) McCarroll, D.; Gagen, M. H.; Loader, N. J.; Robertson, I.; Anchukaitis, K. J.; Los, S.; Young, G. H.; Jalkanen, R.; Kirchhefer, A.; Waterhouse, J. S. Correction of tree ring stable carbon isotope chronologies for changes in the carbon dioxide content of the atmosphere. *Geochim. Cosmochim. Acta* **2009**, *73* (6), 1539−1547.

(16) Treydte, K. S.; Frank, D. C.; Saurer, M.; Helle, G.; Schleser, G. H.; Esper, J. Impact of climate and CO_2 on a millennium-long tree-ring carbon isotope record. *Geochim. Cosmochim. Acta* **2009**, *73* (16), 4635−4647.

(17) Wang, W.; Liu, X.; Shao, X.; Leavitt, S.; Xu, G.; An, W.; Qin, D. A 200 year temperature record from tree ring $\delta^{13}C$ at the Qaidam Basin of the Tibetan Plateau after identifying the optimum method to correct for changing atmospheric CO_2 and $\delta^{13}C$. *J. Geophys. Res.: Biogeosci.* **2011**, *116* (G4), G04022.

(18) Gagen, M.; McCarroll, D.; Loader, N. J.; Robertson, I.; Jalkanen, R.; Anchukaitis, K. J. Exorcising the segment length curse': Summer temperature reconstruction since AD 1640 using non-detrended stable carbon isotope ratios from pine trees in northern Finland. *Holocene* **2007**, *17* (4), 435−446.

(19) Royer, D. L.; Hren, M. T. Carbon isotopic fractionation between whole leaves and cuticle. *Palaios* **2017**, *32* (4), 199−205.

(20) Xu, S. D.; Zhang, J.; Wang, X. X.; Jia, G. D. Catchment environmental change over the 20th Century recorded by sedimentary leaf wax n-alkane $\delta^{13}C$ off the Pearl River estuary. *Sci. China: Earth Sci.* **2016**, *59* (5), 975−980.

(21) Arens, N. C.; Jahren, A. H.; Amundson, R. Can C_3 plants faithfully record the carbon isotopic composition of atmospheric carbon dioxide? *Paleobiology* **2000**, *26*, 137−164.

(22) Kohn, M. J. Carbon isotope discrimination in C_3 land plants is independent of natural variations in pCO_2. *Geochem. Perspect. Lett.* **2016**, *2*, 35−43.

(23) Schubert, B. A.; Jahren, A. H. The effect of atmospheric CO_2 concentration on carbon isotope fractionation in C_3 land plants. *Geochim. Cosmochim. Acta* **2012**, *96*, 29−43.

(24) Schubert, B. A.; Jahren, A. H. Incorporating the effects of photorespiration into terrestrial paleoclimate reconstruction. *Earth-Sci. Rev.* **2018**, *177*, 637−642.

(25) Schubert, B. A.; Jahren, A. H. Global increase in plant carbon isotope fractionation following the Last Glacial Maximum caused by increase in atmospheric pCO_2. *Geology* **2015**, *43* (5), 435−438.

(26) Hobbie, E. A.; Schubert, B. A.; Craine, J. M.; Linder, E.; Pringle, A. Increased C_3 productivity in Midwestern lawns since 1982 revealed by carbon isotopes in *Amanita thiersii*. *J. Geophys. Res.: Biogeosci.* **2017**, *122*, 280−288.

(27) Trahan, M. W.; Schubert, B. A. Temperature-induced water stress in high-latitude forests in response to natural and anthropogenic warming. *Global Change Biol.* **2016**, *22*, 782−791.

(28) Keeling, R. F.; Graven, H. D.; Welp, L. R.; Resplandy, L.; Bi, J.; Piper, S. C.; Sun, Y.; Bollenbacher, A.; Meijer, H. A. Atmospheric evidence for a global secular increase in carbon isotopic discrimination of land photosynthesis. *Proc. Natl. Acad. Sci. U. S. A.* **2017**, *114* (39), 10361−10366.

(29) Tibby, J.; Barr, C.; McInerney, F. A.; Henderson, A. C.; Leng, M. J.; Greenway, M.; Marshall, J. C.; McGregor, G. B.; Tyler, J. J.; McNeil, V. Carbon isotope discrimination in leaves of the broad-leaved paperbark tree, Melaleuca quinquenervia, as a tool for quantifying

DOI: 10.1021/acsearthspacechem.9b00146
ACS Earth Space Chem. 2019, 3, 1966−1973

past tropical and subtropical rainfall. *Global Change Biol.* **2016**, *22* (10), 3474−3486.
(30) Porter, A. S.; Yiotis, C.; Montañez, I. P.; McElwain, J. C. Evolutionary differences in $\Delta^{13}C$ detected between spore and seed bearing plants following exposure to a range of atmospheric O_2:CO_2 ratios; implications for paleoatmosphere reconstruction. *Geochim. Cosmochim. Acta* **2017**, *213*, 517−533.
(31) Abels, H. A.; Lauretano, V.; van Yperen, A. E.; Hopman, T.; Zachos, J. C.; Lourens, L. J.; Gingerich, P. D.; Bowen, G. J. Environmental impact and magnitude of paleosol carbonate carbon isotope excursions marking five early Eocene hyperthermals in the Bighorn Basin, Wyoming. *Clim. Past* **2016**, *12* (5), 1151−1163.
(32) Cui, Y.; Schubert, B. A. Atmospheric pCO_2 reconstructed across five early Eocene global warming events. *Earth Planet. Sci. Lett.* **2017**, *478*, 225−233.
(33) Hare, V. J.; Loftus, E.; Jeffrey, A.; Ramsey, C. B. Atmospheric CO_2 effect on stable carbon isotope composition of terrestrial fossil archives. *Nat. Commun.* **2018**, *9* (1), 252.
(34) Cui, Y.; Schubert, B. A. Towards determination of the source and magnitude of atmospheric pCO_2 change across the early Paleogene hyperthermals. *Global Planet. Change* **2018**, *170*, 120−125.
(35) Wong, C. I.; Breecker, D. O. Advancements in the use of speleothems as climate archives. *Quat. Sci. Rev.* **2015**, *127*, 1−18.
(36) Cui, Y.; Schubert, B. A. Quantifying uncertainty of past pCO_2 determined from changes in C_3 plant carbon isotope fractionation. *Geochim. Cosmochim. Acta* **2016**, *172*, 127−138.
(37) Zhou, B.; Bird, M.; Zheng, H.; Zhang, E.; Wurster, C. M.; Xie, L.; Taylor, D. New sedimentary evidence reveals a unique history of C_4 biomass in continental East Asia since the early Miocene. *Sci. Rep.* **2017**, *7* (1), 170.
(38) Wu, M. S.; Feakins, S. J.; Martin, R. E.; Shenkin, A.; Bentley, L. P.; Blonder, B.; Salinas, N.; Asner, G. P.; Malhi, Y. Altitude effect on leaf wax carbon isotopic composition in humid tropical forests. *Geochim. Cosmochim. Acta* **2017**, *206*, 1−17.
(39) Diefendorf, A. F.; Leslie, A. B.; Wing, S. L. Leaf wax composition and carbon isotopes vary among major conifer groups. *Geochim. Cosmochim. Acta* **2015**, *170*, 145−156.
(40) Zeebe, R. E.; Zachos, J. C.; Dickens, G. R. Carbon dioxide forcing alone insufficient to explain Palaeocene−Eocene Thermal Maximum warming. *Nat. Geosci.* **2009**, *2* (8), 576−580.
(41) Cui, Y.; Kump, L. R.; Ridgwell, A. J.; Charles, A. J.; Junium, C. K.; Diefendorf, A. F.; Freeman, K. H.; Urban, N. M.; Harding, I. C. Slow release of fossil carbon during the Palaeocene-Eocene Thermal Maximum. *Nat. Geosci.* **2011**, *4* (7), 481−485.
(42) Hollis, C. J.; Dunkley Jones, T.; Anagnostou, E.; Bijl, P. K.; Cramwinckel, M. J.; Cui, Y.; Dickens, G. R.; Edgar, K. M.; Eley, Y.; Evans, D.; Foster, G. L.; Frieling, J.; Inglis, G. N.; Kennedy, E. M.; Kozdon, R.; Lauretano, V.; Lear, C. H.; Littler, K.; Meckler, N.; Naafs, B. D. A.; Palike, H.; Pancost, R. D.; Pearson, P.; Royer, D. L.; Salzmann, U.; Schubert, B.; Seebeck, H.; Sluijs, A.; Speijer, R.; Stassen, P.; Tierney, J.; Tripati, A.; Wade, B.; Westerhold, T.; Witkowski, C.; Zachos, J. C.; Zhang, Y. G.; Huber, M.; Lunt, D. J.; et al. The DeepMIP contribution to PMIP4: Methodologies for selection, compilation and analysis of latest Paleocene and early Eocene climate proxy data, incorporating version 0.1 of the DeepMIP database. *Geosci. Model Dev.* **2019**, *12*, 3149−3206.
(43) Foster, G. L.; Royer, D. L.; Lunt, D. J. Future climate forcing potentially without precedent in the last 420 million years. *Nat. Commun.* **2017**, *8*, 14845.
(44) Cranwell, P. A. Diagenesis of free and bound lipids in terrestrial detritus deposited in a lacustrine sediment. *Org. Geochem.* **1981**, *3* (3), 79−89.
(45) Meyers, P. A.; Ishiwatari, R. Lacustrine organic geochemistry—an overview of indicators of organic matter sources and diagenesis in lake sediments. *Org. Geochem.* **1993**, *20* (7), 867−900.
(46) Wakeham, S. G.; Lee, C.; Hedges, J. I.; Hernes, P. J.; Peterson, M. J. Molecular indicators of diagenetic status in marine organic matter. *Geochim. Cosmochim. Acta* **1997**, *61* (24), 5363−5369.
(47) Peters, K.; Walters, C.; Moldowan, J. Biomarkers and Isotopes in Petroleum Exploration and Earth History. *The Biomarker Guide*; Cambridge University Press: Cambridge, U.K., 2005; pp 1−2.
(48) Huang, Y.; Eglinton, G.; Ineson, P.; Latter, P.; Bol, R.; Harkness, D. Absence of carbon isotope fractionation of individual *n*-alkanes in a 23-year field decomposition experiment with Calluna vulgaris. *Org. Geochem.* **1997**, *26* (7−8), 497−501.
(49) Baczynski, A. A.; McInerney, F. A.; Wing, S. L.; Kraus, M. J.; Morse, P. E.; Bloch, J. I.; Chung, A. H.; Freeman, K. H. Distortion of carbon isotope excursion in bulk soil organic matter during the Paleocene-Eocene thermal maximum. *Geol. Soc. Am. Bull.* **2016**, *128*, 1352−1366.
(50) Diefendorf, A. F.; Freeman, K. H.; Wing, S. L.; Graham, H. V. Production of *n*-alkyl lipids in living plants and implications for the geologic past. *Geochim. Cosmochim. Acta* **2011**, *75*, 7472−7485.
(51) Barclay, R. S.; Wing, S. L. Improving the Ginkgo CO_2 barometer: Implications for the early Cenozoic atmosphere. *Earth Planet. Sci. Lett.* **2016**, *439*, 158−171.
(52) Flanagan, L. B.; Brooks, J. R.; Ehleringer, J. R. Photosynthesis and carbon isotope discrimination in boreal forest ecosystems: A comparison of functional characteristics in plants from three mature forest types. *J. Geophys. Res.: Atmos.* **1997**, *102* (D24), 28861−28869.
(53) Leavitt, S.; Newberry, T. Systematics of stable-carbon isotopic differences between gymnosperm and angiosperm trees. *Plant Physiol.* **1992**, *11*, 257−262.
(54) Diefendorf, A. F.; Mueller, K. E.; Wing, S. L.; Koch, P. L.; Freeman, K. H. Global patterns in leaf ^{13}C discrimination and implications for studies of past and future climate. *Proc. Natl. Acad. Sci. U. S. A.* **2010**, *107* (13), 5738−5743.
(55) Barral, A.; Gomez, B.; Fourel, F.; Daviero-Gomez, V.; Lécuyer, C. CO_2 and temperature decoupling at the million-year scale during the Cretaceous Greenhouse. *Sci. Rep.* **2017**, *7*, 8310.
(56) Diefendorf, A. F.; Freeman, K. H.; Wing, S. L.; Currano, E. D.; Mueller, K. E. Paleogene plants fractionated carbon isotopes similar to modern plants. *Earth Planet. Sci. Lett.* **2015**, *429*, 33−44.
(57) Stuiver, M.; Braziunas, T. F. Tree cellulose $^{13}C/^{12}C$ isotope ratios and climatic change. *Nature* **1987**, *328* (6125), 58−60.
(58) Porter, A. S.; Evans-Fitz.Gerald, C.; Yiotis, C.; Montañez, I. P.; McElwain, J. C. Testing the accuracy of new paleoatmospheric CO_2 proxies based on plant stable carbon isotopic composition and stomatal traits in a range of simulated paleoatmospheric O_2:CO_2 ratios. *Geochim. Cosmochim. Acta* **2019**, *259*, 69.
(59) Jia, Y.; Wang, G.; Tan, Q.; Chen, Z. Temperature exerts no influence on organic matter $\delta^{13}C$ of surface soil along the 400 mm isopleth of mean annual precipitation in China. *Biogeosciences* **2016**, *13* (17), 5057−5064.
(60) Lee, X.; Feng, Z.; Guo, L.; Wang, L.; Jin, L.; Huang, Y.; Chopping, M.; Huang, D.; Jiang, W.; Jiang, Q.; Cheng, H. Carbon isotope of bulk organic matter: A proxy for precipitation in the arid and semiarid central East Asia. *Global Biogeochem. Cycles* **2005**, *19* (4), GB4010.
(61) Feng, Z.-D.; Wang, L.; Ji, Y.; Guo, L.; Lee, X.; Dworkin, S. Climatic dependency of soil organic carbon isotopic composition along the S−N Transect from 34 to 52 N in central-east Asia. *Palaeogeogr., Palaeoclimatol., Palaeoecol.* **2008**, *257* (3), 335−343.
(62) Xin, Z.; Liu, M.; Lu, Q.; Busso, C. A.; Zhu, Y.; Li, Z.; Huang, Y.; Li, X.; Luo, F.; Bao, F. Responses of leaf $\delta^{13}C$ and leaf traits to precipitation and temperature in arid ecosystem of northwestern China. *Phyton* **2018**, *87*, 144−155.
(63) Tipple, B. J.; Meyers, S. R.; Pagani, M. Carbon isotope ratio of Cenozoic CO_2: A comparative evaluation of available geochemical proxies. *Paleoceanography* **2010**, *25* (3), PA3202.
(64) Diefendorf, A. F.; Freeman, K. H.; Wing, S. L. A comparison of terpenoid and leaf fossil vegetation proxies in Paleocene and Eocene Bighorn Basin sediments. *Org. Geochem.* **2014**, *71*, 30−42.
(65) Currano, E. D.; Wilf, P.; Wing, S. L.; Labandeira, C. C.; Lovelock, E. C.; Royer, D. L. Sharply increased insect herbivory during the Paleocene-Eocene thermal maximum. *Proc. Natl. Acad. Sci. U. S. A.* **2008**, *105* (6), 1960−1964.

DOI: 10.1021/acsearthspacechem.9b00146
ACS Earth Space Chem. 2019, 3, 1966−1973

(66) Currano, E. D.; Labandeira, C. C.; Wilf, P. Fossil insect folivory tracks paleotemperature for six million years. *Ecol. Monogr.* **2010**, *80* (4), 547−567.
(67) Feild, T. S.; Brodribb, T. J.; Iglesias, A.; Chatelet, D. S.; Baresch, A.; Upchurch, G. R.; Gomez, B.; Mohr, B. A. R.; Coiffard, C.; Kvacek, J.; Jaramillo, C. Fossil evidence for Cretaceous escalation in angiosperm leaf vein evolution. *Proc. Natl. Acad. Sci. U. S. A.* **2011**, *108* (20), 8363−8366.
(68) Vogts, A.; Moossen, H.; Rommerskirchen, F.; Rullkötter, J. Distribution patterns and stable carbon isotopic composition of alkanes and alkanols from plant waxes of African rain forest and savanna C_3 species. *Org. Geochem.* **2009**, *40* (10), 1037−1054.
(69) Dawson, L. A.; Towers, W.; Mayes, R. W.; Craig, J.; Väisänen, R. K.; Waterhouse, E. C. The use of plant hydrocarbon signatures in characterizing soil organic matter. *Geol. Soc. Spec. Publ.* **2004**, *232* (1), 269−276.
(70) Chadwick, M. D.; Chamberlain, D. F.; Knights, B. A.; McAleese, A. J.; Peters, S.; Rankin, D. W.; Sanderson, F. Analysis of leaf waxes as a taxonomic guide to Rhododendron subsection Taliensia. *Ann. Bot.* **2000**, *86* (2), 371−384.
(71) Schwery, O.; Onstein, R. E.; Bouchenak-Khelladi, Y.; Xing, Y.; Carter, R. J.; Linder, H. P. As old as the mountains: The radiations of the Ericaceae. *New Phytol.* **2015**, *207* (2), 355−367.
(72) Snell, K. E.; Thrasher, B. L.; Eiler, J. M.; Koch, P. L.; Sloan, L. C.; Tabor, N. J. Hot summers in the Bighorn Basin during the early Paleogene. *Geology* **2013**, *41* (1), 55−58.
(73) Farquhar, G. D.; Sharkey, T. D. Stomatal conductance and photosynthesis. *Annu. Rev. Plant Physiol.* **1982**, *33* (1), 317−345.
(74) Farquhar, G. D.; O'leary, M.; Berry, J. On the relationship between carbon isotope discrimination and the intercellular carbon dioxide concentration in leaves. *Functional Plant Biology* **1982**, *9* (2), 121−137.
(75) Cernusak, L. A.; Ubierna, N.; Winter, K.; Holtum, J. A.; Marshall, J. D.; Farquhar, G. D. Environmental and physiological determinants of carbon isotope discrimination in terrestrial plants. *New Phytol.* **2013**, *200* (4), 950−965.
(76) Seibt, U.; Rajabi, A.; Griffiths, H.; Berry, J. Carbon isotopes and water use efficiency: Sense and sensitivity. *Oecologia* **2008**, *155* (3), 441−454.
(77) Wang, G.; Li, J.; Liu, X.; Li, X. Variations in carbon isotope ratios of plants across a temperature gradient along the 400 mm isoline of mean annual precipitation in north China and their relevance to paleovegetation reconstruction. *Quat. Sci. Rev.* **2013**, *63*, 83−90.
(78) Fricke, H. C.; Wing, S. L. Oxygen isotope and paleobotanical estimates of temperature and d18O-latitude gradients over North America during the early Eocene. *Am. J. Sci.* **2004**, *304* (7), 612.
(79) Greenwood, D. R.; Wing, S. L. Eocene continental climates and latitudinal temperature gradients. *Geology* **1995**, *23* (11), 1044−1048.
(80) Basu, S.; Ghosh, S.; Sanyal, P. Spatial heterogeneity in the relationship between precipitation and carbon isotopic discrimination in C_3 plants: Inferences from a global compilation. *Global and Planetary Change* **2019**, *176*, 123−131.
(81) Kohn, M. J. Carbon isotope compositions of terrestrial C_3 plants as indicators of (paleo) ecology and (paleo) climate. *Proc. Natl. Acad. Sci. U. S. A.* **2010**, *107* (46), 19691−19695.
(82) Chikaraishi, Y.; Naraoka, H. Compound-specific δD−δ^{13}C analyses of *n*-alkanes extracted from terrestrial and aquatic plants. *Phytochemistry* **2003**, *63* (3), 361−371.
(83) Boudreau, B. P.; Middelburg, J. J.; Sluijs, A.; van der Ploeg, R. Secular variations in the carbonate chemistry of the oceans over the Cenozoic. *Earth Planet. Sci. Lett.* **2019**, *512*, 194−206.
(84) Westerhold, T.; Röhl, U.; Donner, B.; Zachos, J. Global extent of early Eocene hyperthermal events: A new Pacific benthic foraminiferal isotope record from Shatsky Rise (ODP Site 1209). *Paleoceanography and Paleoclimatology* **2018**, *33* (6), 626−642.
(85) Zachos, J. C.; Dickens, G. R.; Zeebe, R. E. An early Cenozoic perspective on greenhouse warming and carbon-cycle dynamics. *Nature* **2008**, *451*, 279−283.
(86) Beerling, D. J.; Royer, D. L. Convergent cenozoic CO_2 history. *Nat. Geosci.* **2011**, *4* (7), 418−420.
(87) Lyons, S. L.; Baczynski, A. A.; Babila, T. L.; Bralower, T. J.; Hajek, E. A.; Kump, L. R.; Polites, E. G.; Self-Trail, J. M.; Trampush, S. M.; Vornlocher, J. R.; Zachos, J. C.; Freeman, K. H. Palaeocene−Eocene Thermal Maximum prolonged by fossil carbon oxidation. *Nat. Geosci.* **2019**, *12* (1), 54.
(88) Lunt, D. J.; Dunkley Jones, T.; Heinemann, M.; Huber, M.; LeGrande, A.; Winguth, A.; Loptson, C.; Marotzke, J.; Roberts, C. D.; Tindall, J.; Valdes, P.; Winguth, C. A model−data comparison for a multi-model ensemble of early Eocene atmosphere−ocean simulations: EoMIP. *Clim. Past* **2012**, *8*, 1717−1736.
(89) Huber, M.; Caballero, R. The early Eocene equable climate problem revisited. *Climate of the Past* **2011**, *7*, 603−633.
(90) Feakins, S. J.; Levin, N. E.; Liddy, H. M.; Sieracki, A.; Eglinton, T. I.; Bonnefille, R. Northeast African vegetation change over 12 my. *Geology* **2013**, *41* (3), 295−298.
(91) Uno, K. T.; Polissar, P. J.; Jackson, K. E.; deMenocal, P. B. Neogene biomarker record of vegetation change in eastern Africa. *Proc. Natl. Acad. Sci. U. S. A.* **2016**, *113* (23), 6355−6363.
(92) Kuypers, M. M.; Pancost, R. D.; Damste, J. S. S. A large and abrupt fall in atmospheric CO_2 concentration during Cretaceous times. *Nature* **1999**, *399* (6734), 342−345.
(93) Romero-Sarmiento, M.-F.; Riboulleau, A.; Vecoli, M.; Versteegh, G. J.-M. Aliphatic and aromatic biomarkers from Gondwanan sediments of Late Ordovician to Early Devonian age: An early terrestrialization approach. *Org. Geochem.* **2011**, *42* (6), 605−617.
(94) Badewien, T.; Vogts, A.; Rullkötter, J. *n*-Alkane distribution and carbon stable isotope composition in leaf waxes of C_3 and C_4 plants from Angola. *Org. Geochem.* **2015**, *89*, 71−79.
(95) Bi, X.; Sheng, G.; Liu, X.; Li, C.; Fu, J. Molecular and carbon and hydrogen isotopic composition of *n*-alkanes in plant leaf waxes. *Org. Geochem.* **2005**, *36* (10), 1405−1417.
(96) Collister, J. W.; Rieley, G.; Stern, B.; Eglinton, G.; Fry, B. Compound-specific δ^{13}C analyses of leaf lipids from plants with differing carbon dioxide metabolisms. *Org. Geochem.* **1994**, *21* (6−7), 619−627.
(97) Conte, M. H.; Weber, J. C.; Carlson, P. J.; Flanagan, L. B. Molecular and carbon isotopic composition of leaf wax in vegetation and aerosols in a northern prairie ecosystem. *Oecologia* **2003**, *135* (1), 67−77.
(98) Duan, Y.; He, J. Distribution and isotopic composition of *n*-alkanes from grass, reed and tree leaves along a latitudinal gradient in China. *Geochem. J.* **2011**, *45* (3), 199−207.
(99) Garcin, Y.; Schefuß, E.; Schwab, V. F.; Garreta, V.; Gleixner, G.; Vincens, A.; Todou, G.; Sene, O.; Onana, J.-M.; Achoundong, G.; Sachse, D. Reconstructing C_3 and C_4 vegetation cover using *n*-alkane carbon isotope ratios in recent lake sediments from Cameroon, Western Central Africa. *Geochim. Cosmochim. Acta* **2014**, *142*, 482−500.
(100) Krull, E.; Sachse, D.; Mügler, I.; Thiele, A.; Gleixner, G. Compound-specific δ^{13}C and δ^{2}H analyses of plant and soil organic matter: A preliminary assessment of the effects of vegetation change on ecosystem hydrology. *Soil Biol. Biochem.* **2006**, *38* (11), 3211−3221.
(101) Schubert, B. A.; Jahren, A. H. Reconciliation of marine and terrestrial carbon isotope excursions based on changing atmospheric CO_2 levels. *Nat. Commun.* **2013**, *4*, 1653.
(102) Fletcher, B. J.; Brentnall, S. J.; Anderson, C. W.; Berner, R. A.; Beerling, D. J. Atmospheric carbon dioxide linked with Mesozoic and early Cenozoic climate change. *Nat. Geosci.* **2008**, *1* (1), 43−48.

DOI: 10.1021/acsearthspacechem.9b00146
ACS Earth Space Chem. 2019, 3, 1966−1973